NASA TN D-271

TECHNICAL NOTE

D-271

ANALYSIS OF ELASTIC-PLASTIC STRESS DISTRIBUTION IN THIN-WALL CYLINDERS AND SPHERES SUBJECTED TO INTERNAL PRESSURE AND NUCLEAR RADIATION HEATING

By Donald F. Johnson

Lewis Research Center
Cleveland, Ohio

NATIONAL AERONAUTICS AND SPACE ADMINISTRATION

WASHINGTON

April 1960

NATIONAL AERONAUTICS AND SPACE ADMINISTRATION

TECHNICAL NOTE D-271

ANALYSIS OF ELASTIC-PLASTIC STRESS DISTRIBUTION IN THIN-WALLED CYLINDERS AND SPHERES SUBJECTED TO INTERNAL PRESSURE AND NUCLEAR RADIATION HEATING

By Donald F. Johnson

SUMMARY

The steady-state elastic-plastic stress distributions in cylindrical and spherical vessels subjected to internal pressure, symmetrical nuclear heating, and inside-wall cooling were calculated. A finite-difference method combined with a technique of successive approximations was used. The material properties used were those of Inconel X, but the method used is applicable to any material. For given values of pressure load (pressure times radius) and heat flux, there is a minimum possible strain for each vessel configuration that occurs at a particular wall thickness for each configuration. Furthermore, for a given value of pressure load, the minimum strain for different heat fluxes occurs at essentially the same wall thickness. The optimum thicknesses and corresponding strains for the sphere were approximately half those for the cylinder for the same loads.

INTRODUCTION

A nuclear-rocket component that presents unique design problems is the pressure shell surrounding the reactor core. Not only is heat generated within the shell by gamma and neutron radiation, but also the inside surface of the shell is heated by thermal radiation from the neutron shield or reflector. Since weight saving is extremely important in any rocket vehicle, it is desirable to reduce the thickness of the shield as much as possible. When this is done the pressure shell is subjected to higher nuclear heat flux. Cooling of the shell will therefore be a necessity. The simplest arrangement is to cool the inside surface with the propellant before it passes through the reactor.

With any cooling method, thermal stresses will be developed because of nonuniform temperatures within the shell. In general, these stresses will increase as the temperature gradient increases; and the gradient

varies with the thickness of the shell and the gamma-neutron heat flux. In addition to increasing stress, the increase in average temperature level causes a lowering of the mechanical-strength properties of the shell material. The design procedure for a reactor pressure shell with high heat flux from nuclear radiation is therefore unique in that the safety factor cannot always be increased by making the shell thicker, since the thicker shell might result in added heat generation and a reduction in strength. The design procedure should therefore incorporate a method of finding whether an optimum shell thickness exists.

There is little information in the literature on reactor pressure-shell design. Reference 1 discusses the possibility of a pressure-shell failure due to sudden excursions in the reactor. The conclusion is drawn that the containment potential of a reactor pressure shell is substantially improved by the strain-energy absorption obtained by large plastic deformation. It seems probable that plastic flow will have to be considered in any reactor pressure-shell design where there is a high heat flux from nuclear radiation.

The complete design for a reactor pressure shell for a nuclear rocket would include design of the exhaust nozzle as well as the remainder of the pressure shell, which could consist of a sphere or a cylindrical portion with a hemispherical end. As a first approach to such a design study, this report presents an analytical method including plastic flow for designing a spherical shell and a cylindrical shell with a hemispherical end. The nozzle is not considered. The analysis considers cooling on the inside surface of the pressure-vessel wall only. The method used is based on the finite-difference approach of references 2 and 3 and the successive-approximation technique of reference 4. The analysis was made using Inconel X as the vessel material. A range of heat fluxes up to 950 watts per cubic centimeter and a range of pressure loads (product of pressure times radius) from 18,000 to 42,000 pounds per inch were considered.

SYMBOLS

A_j	conductivity constants, Btu/(hr)(sq ft)($^{\circ}F^2$/ft)
a	inside radius (station 1), in.
B_j	conductivity constants, Btu/(hr)(sq ft)($^{\circ}$F/ft)
b	outside radius (station 20), in.
C_1, C_2	strain constants
E	elastic modulus, psi
h_n	$r_n - r_{n-1}$, in.

k	conductivity, Btu/(hr)(sq ft)(^{o}F/ft)
l	length of cylinder, in.
p	internal pressure, psi
Q	heat flow, watts
Q/V	nuclear-radiation heat flux, w/cc
r	radial distance, in.
T	temperature above arbitrary zero, ^{o}F
t	thickness, in.
u	radial displacement, in.
α	coefficient of thermal expansion, in./(in.)(^{o}F)
β	conversion factor, 2.54^{3} $cm^{3}/in.^{3}$
γ	conversion factor, $0.0244 \frac{(watt)(ft)(hr)}{(Btu)(in.)}$
ϵ	total strain, in./in.
μ	Poisson's ratio
σ	stress, psi

Subscripts:

a	inside radius
c	cylinder
e	equivalent
ep	equivalent plastic
et	equivalent total
i	inside surface
j	1, 2
n	n^{th} point
o	outside surface

p	plastic
r	radial
s	sphere
z	longitudinal
θ	tangential

ANALYTICAL PROCEDURE

Analysis of Cylinder

An analysis was made on a long circular cylinder subject to the following assumptions:

(1) The cylinder material is linearly elastic up to the elastic limit; beyond this point, plastic flow occurs.

(2) Axial symmetry exists.

(3) Generalized plane strain exists in that the axial strain ϵ_z does not vary in the radial direction.

(4) The inside wall is cooled to 100° F.

(5) Steady-state conditions are present as far as the heat flow is concerned.

(6) Calculations are made at a sufficient distance from the ends so that end conditions are negligible.

(7) The cylinder is subjected to an internal pressure and is without axial restraint.

(8) The coefficient of thermal expansion, the conductivity, and the modulus of elasticity vary in a known manner with temperature.

(9) Poisson's ratio is a constant ($\mu = 0.3$).

(10) The deformation theory of plasticity with the von Mises yield condition is used.

Determination of Stress and Strain Distribution

The determination of stresses and strains in a long cylinder follows the usual treatment for plane strain problems. The equilibrium equation

is given by

$$\frac{d\sigma_r}{dr} + \frac{\sigma_r - \sigma_\theta}{r} = 0 \tag{1}$$

The compatibility equation is

$$\frac{d\epsilon_\theta}{dr} + \frac{\epsilon_\theta - \epsilon_r}{r} = 0 \tag{2}$$

and the stress-strain relations are

$$\left.\begin{aligned} \epsilon_r &= \frac{1}{E}\left[\sigma_r - \mu(\sigma_\theta + \sigma_z)\right] + \alpha T + \epsilon_{r,p} \\ \epsilon_\theta &= \frac{1}{E}\left[\sigma_\theta - \mu(\sigma_r + \sigma_z)\right] + \alpha T + \epsilon_{\theta,p} \\ \epsilon_z &= \frac{1}{E}\left[\sigma_z - \mu(\sigma_\theta + \sigma_r)\right] + \alpha T + \epsilon_{z,p} \end{aligned}\right\} \tag{3}$$

Writing equation (2) in terms of stresses by the use of equations (3) gives

$$\frac{d}{dr}\left(\frac{1}{E}\sigma_\theta - \frac{\mu}{E}\sigma_r - \frac{\mu}{E}\sigma_z + \alpha T + \epsilon_{\theta,p}\right) = \frac{1+\mu}{Er}(\sigma_r - \sigma_\theta) + \frac{\epsilon_{r,p} - \epsilon_{\theta,p}}{r} \tag{4}$$

Also, solving the last of equations (3) for σ_z and substituting into equation (4) give

$$\frac{d}{dr}\left[\frac{1}{E}\sigma_\theta - \frac{\mu}{E}\sigma_r - \mu\epsilon_z - \frac{\mu^2}{E}(\sigma_r + \sigma_\theta) + \mu\alpha T + \mu\epsilon_{z,p} + \alpha T + \epsilon_{\theta,p}\right]$$

$$= \frac{1+\mu}{Er}(\sigma_r - \sigma_\theta) + \frac{\epsilon_{r,p} - \epsilon_{\theta,p}}{r} \tag{5}$$

For the generalized plane strain problem, ϵ_z is a constant and is determined from the axial loading on the cylinder as follows:

$$\int_a^b \sigma_z r\, dr = \frac{a^2 p}{2} \tag{6}$$

or

$$\int_a^b \left[E\epsilon_z + \mu(\sigma_r + \sigma_\theta) - E\alpha T - E\epsilon_{z,p}\right] r\, dr = \frac{a^2 p}{2}$$

Therefore,

$$\epsilon_z = \frac{\frac{a^2 p}{2} - \int_a^b \left[\mu(\sigma_r + \sigma_\theta) - E\alpha T - E\epsilon_{z,p}\right] r\, dr}{\int_a^b Er\, dr} \qquad (7)$$

Substituting equation (7) in equation (5) gives a pair of simultaneous differential equations, (1) and (5), that can be solved for σ_r and σ_θ. In the elastic case ($\epsilon_{r,p}$, $\epsilon_{\theta,p}$, and $\epsilon_{z,p}$ all zero), these equations are linear and can be solved by a variety of ways - for example, the finite-difference method of reference 2. For the case of plastic flow, however, the plastic-flow terms are nonlinear functions of the dependent variables (the stresses), and the solution becomes more difficult.

In the present paper, equations (1) and (5) were solved by converting them to finite-difference form, as was done in references 2 and 3 and described in detail in appendix A, and then solving these finite-difference equations by the method of successive approximations as given in reference 4. Briefly, this method consists of first assuming some plastic-strain distribution (such as zero everywhere). Since the plastic-flow terms in equations (1) and (5) are now known quantities, these equations can be solved by the finite-difference method. This gives a first approximation to the stress and strain distribution. From this first approximation a better approximation is computed for the plastic strains by means of the stress-strain relations in the plastic range subsequently discussed. These new values of the plastic strains are put into equations (1) and (5), and these equations are solved again by the finite-difference method. This process is then repeated continuously until convergence is obtained; that is, the difference between the distributions computed for two successive iterations is as small as desired.

In order to determine the new values of the plastic strains at any point of the preceding calculation, a stress-strain relation for triaxial stresses is needed. It was assumed in making these calculations that the deformation theory of plasticity and the von Mises yield criterion are valid. On this basis it is shown in appendix B that the plastic strains can be computed from the total strains by means of the following equations:

$$\left.\begin{aligned} \epsilon_{r,p} &= \frac{\epsilon_{ep}}{3\epsilon_{et}} (2\epsilon_r - \epsilon_\theta - \epsilon_z) \\ \epsilon_{\theta,p} &= \frac{\epsilon_{ep}}{3\epsilon_{et}} (2\epsilon_\theta - \epsilon_r - \epsilon_z) \\ \epsilon_{z,p} &= -\epsilon_{r,p} - \epsilon_{\theta,p} \end{aligned}\right\} \tag{8}$$

where

$$\epsilon_{et} \equiv \frac{\sqrt{2}}{3} \sqrt{(\epsilon_r - \epsilon_\theta)^2 + (\epsilon_r - \epsilon_z)^2 + (\epsilon_z - \epsilon_\theta)^2} \tag{9}$$

and ϵ_{ep} is related to ϵ_{et} through the stress-strain curve of the material by the following relation:

$$\epsilon_{et} = \frac{2}{3} \frac{\sigma_e}{E} (1 + \mu) + \epsilon_{ep} \tag{10}$$

where the equivalent stress σ_e and the equivalent plastic strain ϵ_{ep} are shown on the typical stress-strain curve (fig. 1), which was obtained from unpublished NASA data. Using relation (10) together with the stress-strain curve for the material, it is possible to plot ϵ_{ep} against ϵ_{et} as shown in figure 2. This figure can now be used together with equations (8) to calculate the values of the plastic strains.

The method of calculation can now be summarized as follows:

(1) Assume values for the plastic strains such as $\epsilon_{r,p} = \epsilon_{\theta,p} = 0$ everywhere.

(2) Solve equations (1) and (5) by the finite-difference method described in appendix A.

(3) Calculate the total strains by means of equations (3).

(4) Calculate the equivalent total strain ϵ_{et} from equation (9).

(5) Read ϵ_{ep} from figure 2.

(6) Calculate $\epsilon_{r,p}$, $\epsilon_{\theta,p}$, and $\epsilon_{z,p}$ from equations (8).

(7) Using these values in equations (1) and (5), go back to step (2).

(8) Continue until convergence is obtained.

Determination of Temperature Distribution

Before equations (1) and (5) can be solved, it is necessary to know the temperature distribution. The heat generated within the wall due to neutron and gamma radiation heating is

$$Q = \pi l \beta \frac{Q}{V} (r_o^2 - r^2) \tag{11}$$

This same amount of heat is transferred by conduction towards the inner wall:

$$Q = 2\pi r l \gamma k \frac{dT}{dr} \tag{12}$$

Therefore,

$$k\, dT = \frac{\beta}{\gamma} \frac{Q}{V} \frac{(r_o^2 - r^2)}{2r} dr \tag{13}$$

where the conversion factors β and γ have the values

$$\beta = \left(\frac{2.54 \text{ cm}}{\text{in.}}\right)^3$$

$$\gamma = 0.0244 \frac{(\text{watt})(\text{ft})(\text{hr})}{(\text{Btu})(\text{in.})}$$

From figure 3 it can be seen that the variation of k with temperature can be approximated by two straight lines. Therefore, $k = A_1T + B_1$ for the part of the curve from A to B, and $k = A_2T + B_2$ from B to C. Integrating from r_i to r and using appropriate values of A and B for the portion of the curve integrated over, the left side of equation (13) becomes

$$\int_T^{T_o} (A_jT + B_j)dT = \frac{A_j}{2} (T_o^2 - T^2) + B_j(T_o - T)$$

and the right side of equation (13) becomes

$$\frac{1}{2} \frac{\beta}{\gamma} \frac{Q}{V} \int_r^{r_o} \frac{(r_o^2 - r^2)}{r} dr = \frac{\beta}{2\gamma} \frac{Q}{V} \left[r_o^2 \ln \frac{r_o}{r} - \frac{1}{2} (r_o^2 - r^2)\right] \equiv f_c(r)$$

Combining the two sides of the equation and simplifying give

$$T^2 + \frac{2B_j}{A_j} T - T_o^2 - \frac{2B_j}{A_j} T_o + \frac{2f_c(r)}{A_j} = 0 \tag{14}$$

Using the condition that when $r = r_i$, $T = T_i$, equation (14) can be solved for T_o:

$$T_o = -\frac{B_j}{A_j} \pm \sqrt{\left(T_i + \frac{B_j}{A_j}\right)^2 + \frac{2f_c(r_i)}{A_j}}$$

The temperature at any radius r, T_r is obtained by solving (14) for T:

$$T_r = -\frac{B_j}{A_j} \pm \sqrt{\left(T_o + \frac{B_j}{A_j}\right)^2 - \frac{2f_c(r)}{A_j}}$$

In order for the temperature to be positive, the plus sign is used with the radical.

Analysis of Sphere

Because of the symmetry of a sphere, the complete stress state is defined where the radial and tangential stresses are known at any radius. The assumptions enumerated for the cylinder also apply to the sphere, with the exception of those that apply to the cylinder only by virtue of its geometry. The procedure is the same as for the cylinder with slight modifications. The equilibrium and compatibility relations are different, and all of the equations are simplified because of the spherical symmetry, which reduces the number of stresses and strains from three to two. The complete analysis is given in appendix C, and the analysis of the temperature distribution is given in appendix D.

COMPUTATION

The curve of ϵ_{ep} against ϵ_{et} in figure 2 can be approximated by two straight lines, one from A to B and the other from B to C. In the analysis, therefore, the following relation was used:

$$\epsilon_{ep} = C_1 + C_2\epsilon_{et}$$

where C_1 and C_2 changed for each portion of the curve. It was necessary to use different curves for different temperatures. Because of the scatter in the experimental data and the error involved in drawing the best curve through the points, the linear assumption was considered justified and within the overall error of the input data. For ease of programming, a linear interpolation was used for the value of C_1 and C_2 between $T = 180^\circ$ and 910° F. Above 910° F, which was the maximum temperature for which stress-strain data were available, a linear extrapolation was used. For a material for which the slope of the plastic

portion of the stress-strain curve was not fairly constant, other relations would have to be used. For convenience of computation, the curves of coefficient of expansion and conductivity against temperature were approximated by two straight lines each, as shown in figure 3. The curve of elastic modulus against temperature was approximated by a quadratic equation (fig. 3).

An IBM 653 electronic computer was used to make the calculations. It was determined that, when two successive values of ϵ_r at the inside surface differed by less than 1 in the sixth place, the convergence was sufficient, since, at the most, three significant figures are used in the graphical plots. With further iterations ϵ_r changed no further. The changes in the stress were always at least an order of magnitude less than the changes in strain. Therefore, the sixth-place convergence criterion was also sufficient for the stresses.

RESULTS AND DISCUSSION

Optimum Thickness

The variables pertinent to the calculation of optimum thickness were radius, thickness, heat flux, and pressure. Figure 4 shows the equivalent total strain at the inside wall as a function of thickness for different values of heat flux and pressure load (pressure times radius). It is obvious that there is an optimum thickness with respect to minimum strain. This optimum arises from the fact that decreasing the thickness causes an increase in the stress due to pressure, while increasing the thickness causes an increase in the temperature gradient and hence an increase in thermal strain. The minimum strain is relatively independent of thickness except as the heat flux becomes low. At low values of heat flux the thickness may be increased to lower the strain level. Since the thermal gradients will be low, the problem is reduced to a standard pressure-vessel calculation. However, when it is realized that weight is at a premium and therefore a minimum thickness is a necessity, it can be seen that the optimum thickness is essentially the same for all values of heat flux.

Excursions in Heat Flux

Figure 4 is also a graphical illustration of the effect of excursions in heat flux. It can be seen that a large range of heat fluxes can be tolerated at low values of pressure load. That is, the equivalent total strain increases at about 1/4 the rate of the heat flux. At the larger pressure load of 42,000 pounds per inch, the ratio drops to about 1, although the strain still increases at a slightly lower rate than the heat flux.

Pressure Excursions

Pressure excursions are also possible in a nuclear reactor. Figure 5 shows results of excursions of ±10 percent. It can be seen that the equivalent total strain for optimum thickness rises 25 percent for the cylinder and 40 percent for the sphere when the pressure rises from 1000 to 1100 pounds per square inch. It is apparent that a change of thickness and/or pressure of up to 10 percent does not cause increases in equivalent total strain great enough to lead to failure within the range of parameters investigated. Therefore, if pressure excursions are expected, one should design for overpressure.

Distributions of Stress and Strain

For a given material the main parameters affecting the severity of the temperature gradient were heat flux, thickness, and, to a lesser extent, radius. Two typical temperature distributions through the cylinder wall are shown in figure 6(a). The data for the two curves are for the two extreme conditions (with regard to strain) of pressure load and heat flux from figure 4(a). It can be seen in figures 6(b) and (c) that the maximum values of stress and strain are at the inside wall. This is due to the fact that the thermal strain is compressive at the outside surface and tensile at the inside surface, whereas the strain due to pressure is tensile throughout the thickness. Thus, the thermal and pressure strains tend to cancel at the outside surface and add at the inside surface. It can also be seen that the tangential stress is the largest of the stresses. For simplicity, only the equivalent total strain and the tangential stress at the inside wall are discussed. The radial stress σ_r was not plotted, since its maximum value, which is equal to the pressure, is less than 2 percent of the other two stresses.

Design Curves

Figure 7 is a series of curves summarizing the quantitative results of this investigation. The equivalent total strain at the inside wall is plotted as a function of the heat flux. Each curve is for a given pressure load. The existence of a single curve for each value of pressure load was verified by varying the pressure and radius but keeping the product constant. Several points are plotted showing this verification. The two intermediate curves in figure 7(a) at pressure loads of 36,000 and 24,000 pounds per inch were obtained by cross-plotting. One calculated data point on each curve indicates that the technique was sufficiently accurate. The thicknesses used were the optimum thicknesses for the particular pressure load. Figure 7 also shows that, for smaller values of pressure load, larger heat fluxes can be tolerated with consequent equal or smaller equivalent total strains.

If the value of pressure load for each curve is divided by the corresponding optimum thickness, the average hoop stress is obtained. This average hoop stress varies in the cylinder from about 100,000 psi at a pressure load of 18,000 pounds per inch to 110,500 psi at a pressure load of 42,000 pounds per inch. The tangential stress in the sphere is equal to $pr/2t$. This varies from 90,000 to about 96,000 psi for pressure loads from 18,000 to 42,000 pounds per inch. This allows the designer to calculate a rough value of t for a given hoop stress. However, to get the corresponding strains, it would be necessary to go through the complete analysis. There is only about a ± 5-percent variation in average stress, while the average strains vary from below the elastic limit to about 2.6 percent, depending on the heat flux. This is logical when one observes the shape of the stress-strain curve in figure 1. It can be seen that in the plastic region large changes in strain result in relatively small changes in stress.

The curves in figure 7 actually constitute a set of design curves. The designer can quickly determine an optimum thickness from the curves for his particular pressure load and allowable equivalent total strain. The maximum heat flux that can be tolerated can be read from the abscissa. These curves were obtained for a particular method of cooling. If the designer finds himself limited to either too small a strain or too small a heat flux, or both, it is apparent that a better cooling method, such as internal-wall cooling, would have to be employed and incorporated in the analysis.

Spherical Tank

A spherical tank could be used if the length-diameter ratio of the core were equal or close to unity. However, the diameter of a spherical tank would have to be equal to $\sqrt{2}$ times the diameter of a cylindrical tank. The results of comparing the equivalent total strains of a cylinder and an equivalent sphere found by multiplying the pressure load in the cylinder by $\sqrt{2}$ are shown in table I. It can be seen that the strains in the sphere are only about 70 to 80 percent of those in the cylinder.

Material Properties

The choice of the material for a nuclear-reactor pressure shell depends on several factors. Of primary importance is high tensile strength at high temperatures. Coupled with this, a reasonable amount of ductility is necessary. Data at temperatures up to about 1400° F were available for Inconel X. Its tensile strength up to 1350° F was better than that of the available high-temperature steels, and much more complete stress-strain data at high temperatures were available. Therefore, Inconel X was chosen for the purposes of this investigation. However, other materials such as aluminum or titanium might be applicable.

In order to obtain the stress and strain distributions for a material other than Inconel X, it would be necessary to run a complete analysis using the mechanical and physical constants for that material. This was beyond the scope of this report. However, an attempt was made to determine the effect of varying some of the material properties while holding the others constant at the values for Inconel X. Table II gives the equivalent total strain and the tangential stress at the inside wall for the two extreme strain cases that have been used previously for comparisons. Also given in the table are values obtained at conductivities varying from 10 Btu/(hr)(sq ft)($^{\circ}$F/ft) at 0° F to about 16.5 at 1200° F, and from 6.8 at 0° F to 14.2 at 1200° F. Coefficients of expansion varying from 9.1 inch per inch per $^{\circ}$F at 0° F to 10 at 1400° F and from 5.2 at 0° F to 6.8 at 1400° F were considered. These values encompass the range that might be encountered with several high-temperature alloys. It can be seen that a considerable variation of α and k makes a rather small difference in the stress and strain values.

Hemispherical End on Cylindrical Tank

For a hemispherical end on a cylindrical tank, calculations were made using the analysis of the sphere with the thickness equal to the optimum thickness of the cylinder, thus giving results for the case of equal thickness in the cylinder and the end. It was established that the strains in the hemispherical end were less than those in the cylinder by about 30 percent. The results of three calculations are shown in table III. Thus, a hemispherical end on a cylindrical pressure vessel of the same thickness as the cylinder would be subjected to 30-percent less strain than the cylinder. There are additional strains at the joint between the cylinder and hemisphere due to discontinuities, but calculation of these is beyond the scope of this report.

CONCLUSIONS

For the analysis conducted herein on an Inconel X reactor pressure vessel with internally cooled walls, the following conclusions can be drawn:

1. For given values of pressure load and heat flux, there is a minimum possible strain that occurs at a particular wall thickness.

2. For a given value of pressure load, the minimum equivalent total strain for the range of heating fluxes investigated will occur at essentially the same wall thickness.

3. The average tangential stress for optimum wall thickness is essentially constant for a given material, varying only about ±5 percent throughout the range of heat flux and pressure load investigated; but the strain varies considerably.

4. Variation of conductivity and coefficient of expansion does not change the trend of the results; but the strains may be affected, particularly at high values of heat flux and thickness.

5. A pressure excursion of ±10 percent would be tolerable over the range of heat flux and pressure load investigated.

6. The equivalent total strain increases at a lower rate than the heat flux over the range of heat flux investigated.

7. In the case of a reactor core of length-diameter ratio equal to unity, a spherical containment vessel would be subjected to from 70 to 80 percent of the strain of a cylindrical containment vessel.

Lewis Research Center
National Aeronautics and Space Administration
Cleveland, Ohio, December 21, 1959

APPENDIX A

DETERMINATION OF STRESS AND STRAIN DISTRIBUTION IN CYLINDER

Equations (1) and (5) were solved by the method used in reference 3 with appropriate changes to apply to a cylinder instead of a disk.

In the finite-difference method, a number of discrete point stations are chosen along the radius of the cylinder. It is assumed that at each of these points the plastic strains, the temperature, and the quantities E, α, and μ are known, and also that the values of these quantities can be approximated midway between these point stations. An explanation of the determination of the preceding quantities is given in the body of the report. Using middle differences, let

$$\frac{d\sigma}{dr} = \frac{\sigma_n - \sigma_{n-1}}{r_n - r_{n-1}} \qquad \text{and} \qquad \sigma = \frac{\sigma_n + \sigma_{n-1}}{2}$$

Substituting this (and similar relations for other quantities) into equations (1) and (5),

$$C_n\sigma_{r,n} - D_n\sigma_{\theta,n} = F_n\sigma_{r,n-1} + G_n\sigma_{\theta,n-1} \tag{A1}$$

$$C'_n\sigma_{r,n} + D'_n\sigma_{\theta,n} = F'_n\sigma_{r,n-1} + G'_n\sigma_{\theta,n-1} + H'_n + P'_n \tag{A2}$$

where

$$C_n = \frac{1}{h_n} + \frac{1}{2r_n} \qquad C'_n = -\frac{\mu}{(hE)_n} - \frac{\mu^2}{(hE)_n} - \frac{1+\mu}{2E_nr_n}$$

$$D_n = \frac{1}{2r_n} \qquad D'_n = \frac{1}{(hE)_n} - \frac{\mu^2}{(hE)_n} + \frac{1+\mu}{2E_nr_n}$$

$$F_n = \frac{1}{h} - \frac{1}{2r_{n-1}} \qquad F'_n = -\frac{\mu}{(hE)_{n-1}} - \frac{\mu^2}{(hE)_{n-1}} + \frac{1+\mu}{2E_{n-1}r_{n-1}}$$

$$G_n = \frac{1}{2r_{n-1}} \qquad G'_n = \frac{1}{(hE)_{n-1}} - \frac{\mu^2}{(hE)_{n-1}} - \frac{1+\mu}{2E_{n-1}r_{n-1}}$$

$$H'_n = -\frac{1+\mu}{h_n}\left[(\alpha T)_n - (\alpha T)_{n-1}\right]$$

$$P'_n = \left(-\frac{1}{h_n} - \frac{1}{2r_n} + \frac{\mu}{h_n}\right)\epsilon_{\theta,p,n} + \left(\frac{1}{2r_n} + \frac{\mu}{h_n}\right)\epsilon_{r,p,n} + \left(\frac{1}{h_n} - \frac{1}{2r_{n-1}} - \frac{\mu}{h_n}\right)\epsilon_{\theta,p,n-1}$$

$$+\left(\frac{1}{2r_{n-1}} - \frac{\mu}{h_n}\right)\epsilon_{r,p,n-1}$$

Considering the linear nature of equations (A1) and (A2) and the possibility of successive application of these equations in going from station to station, it follows that the stresses at any station can ultimately be expressed in linear terms of the stresses at any other station. For convenience, the stresses at all stations are expressed in terms of the tangential stress at the inner radius $\sigma_{\theta,a}$; thus,

$$\sigma_{r,n} = A_{r,n}\sigma_{\theta,a} + B_{r,n} \tag{A3}$$

$$\sigma_{\theta,n} = A_{\theta,n}\sigma_{\theta,a} + B_{\theta,n} \tag{A4}$$

$$\sigma_{r,n-1} = A_{r,n-1}\sigma_{\theta,a} + B_{r,n-1} \tag{A5}$$

$$\sigma_{\theta,n-1} = A_{\theta,n-1}\sigma_{\theta,a} + B_{\theta,n-1} \tag{A6}$$

Substituting these values of $\sigma_{r,n}$, $\sigma_{\theta,n}$, $\sigma_{r,n-1}$, and $\sigma_{\theta,n-1}$ into equations (A1) and (A2),

$$(C_nA_{r,n} - D_nA_{\theta,n} - F_nA_{r,n-1} - G_nA_{\theta,n-1})\sigma_{\theta,a} + (C_nB_{r,n} - D_nB_{\theta,n} - F_nB_{r,n-1} - G_nB_{\theta,n-1}) = 0 \tag{A7}$$

$$(C'_nA_{r,n} - D'_nA_{\theta,n} - F'_nA_{r,n-1} - G'_nA_{\theta,n-1})\sigma_{\theta,a} + (C'_nB_{r,n} - D'_nB_{\theta,n} - F'_nB_{r,n-1} - G'_nB_{\theta,n-1} - H'_n - P'_n) = 0 \tag{A8}$$

In equations (A7) and (A8), the stress $\sigma_{\theta,a}$ is completely arbitrary, since it depends only upon the boundary conditions and not on the equations of elasticity. Thus, the equations are valid for any value of $\sigma_{\theta,a}$. For this to be true, the terms in the parentheses must equal zero. Therefore,

$$\left.\begin{aligned} C_nA_{r,n} - D_nA_{\theta,n} - F_nA_{r,n-1} - G_nA_{\theta,n-1} &= 0 \\ C_nB_{r,n} - D_nB_{\theta,n} - F_nB_{r,n-1} - G_nB_{\theta,n-1} &= 0 \\ C'_nA_{r,n} - D'_nA_{\theta,n} - F'_nA_{r,n-1} - G'_nA_{\theta,n-1} &= 0 \\ C'_nB_{r,n} - D'_nB_{\theta,n} - F'_nB_{r,n-1} - G'_nB_{\theta,n-1} + H'_n + P'_n &= 0 \end{aligned}\right\} \tag{A9}$$

Solving these four equations simultaneously for $A_{r,n}$, $A_{\theta,n}$, $B_{r,n}$, and $B_{\theta,n}$,

$$\left.\begin{aligned} A_{r,n} &= KA_{r,n-1} + LA_{\theta,n-1} \\ A_{\theta,n} &= K'A_{r,n-1} + L'A_{\theta,n-1} \\ B_{r,n} &= KB_{r,n-1} + LB_{\theta,n-1} + M \\ B_{\theta,n} &= K'B_{r,n-1} + L'B_{\theta,n-1} + M' \end{aligned}\right\} \qquad \text{(A10)}$$

where

$$K_n = \frac{D_n'F_n + D_nF_n'}{C_nD_n' + C_n'D_n} \qquad K_n' = \frac{C_nF_n' - C_n'F_n}{C_nD_n' + C_n'D_n}$$

$$L_n = \frac{D_n'G_n + D_nG_n'}{C_nD_n' + C_n'D_n} \qquad L_n' = \frac{C_nG_n' - C_n'G_n}{C_nD_n' + C_n'D_n}$$

$$M_n = \frac{D_n(H_n' + P_n')}{C_nD_n' + C_n'D_n} \qquad M_n' = \frac{C_n(H_n' + P_n')}{C_nD_n' + C_n'D_n}$$

At $r = a$ (station 1, inside surface), $\sigma_{r,a} = -p$ (boundary condition) and $\sigma_{\theta,n} = \sigma_{\theta,a}$. Substituting in equations (A3) and (A4),

$$-p = A_{r,a}\sigma_{\theta,a} + B_{r,a}$$

$$\sigma_{\theta,a} = A_{\theta,a}\sigma_{\theta,a} + B_{\theta,a}$$

These equations are true regardless of the value of $\sigma_{\theta,a}$. Therefore,

$$\left.\begin{aligned} B_{\theta,a} &= 0 \\ A_{\theta,a} &= 1 \\ A_{r,a} &= 0 \\ B_{r,a} &= -p \end{aligned}\right\} \qquad \text{(A11)}$$

The radial stress at the outside surface ≈ 0 (boundary condition). Therefore,

$$\sigma_{r,b} = 0 = A_{r,b}\sigma_{\theta,a} + B_{r,b}$$

or

$$\sigma_{\theta,a} = - \frac{B_{r,b}}{A_{r,b}} \tag{A12}$$

From the known coefficients at the first station (eq. (A11)), the coefficients at all other stations can be determined progressively by successive applications of equation (A10). When all of the coefficients have been determined, the unknown $\sigma_{\theta,a}$ can be determined from equation (A12). Then the radial and tangential stresses can be determined using equations (A3) and (A4).

APPENDIX B

CALCULATION OF PLASTIC STRAINS

This appendix is taken from reference 4, appendix I.

The deformation theory of plasticity is used with the three usual assumptions that the directions of the principal strains coincide with the directions of the principal stresses, that the ratios of the principal shear strains are equal to the ratios of the principal shear stresses, and that the volume remains constant in the plastic range. These assumptions imply

$$\left.\begin{aligned} \frac{\epsilon_r - \epsilon_\theta}{\sigma_r - \sigma_\theta} = \frac{\epsilon_r - \epsilon_z}{\sigma_r - \sigma_z} = \frac{\epsilon_\theta - \epsilon_z}{\sigma_\theta - \sigma_z} = K_1 \\ \epsilon_{r,p} + \epsilon_{\theta,p} + \epsilon_{z,p} = 0 \end{aligned}\right\} \tag{B1}$$

By substituting the stress-strain relations,

$$\left.\begin{aligned} \epsilon_r &= \frac{1}{E}\left[\sigma_r - \mu(\sigma_\theta + \sigma_z)\right] + \epsilon_{r,p} + \alpha T \\ \epsilon_\theta &= \frac{1}{E}\left[\sigma_\theta - \mu(\sigma_r + \sigma_z)\right] + \epsilon_{\theta,p} + \alpha T \\ \epsilon_z &= \frac{1}{E}\left[\sigma_z - \mu(\sigma_r + \sigma_\theta)\right] + \epsilon_{z,p} + \alpha T \end{aligned}\right\} \tag{B2}$$

into the first of equations (B1), it can also be shown that

$$\frac{\epsilon_{r,p} - \epsilon_{\theta,p}}{\sigma_r - \sigma_\theta} = \frac{\epsilon_{r,p} - \epsilon_{z,p}}{\sigma_r - \sigma_z} = \frac{\epsilon_{\theta,p} - \epsilon_{z,p}}{\sigma_\theta - \sigma_z} = K_2 \tag{B3}$$

where

$$K_1 = K_2 + \frac{1 + \mu}{E} \tag{B4}$$

Define

$$\left.\begin{aligned}
\sigma_e &= \frac{1}{\sqrt{2}} \sqrt{(\sigma_r - \sigma_\theta)^2 + (\sigma_r - \sigma_z)^2 + (\sigma_\theta - \sigma_z)^2} \\
\epsilon_{ep} &= \frac{\sqrt{2}}{3} \sqrt{(\epsilon_{r,p} - \epsilon_{\theta,p})^2 + (\epsilon_{r,p} - \epsilon_{z,p})^2 + (\epsilon_{\theta,p} - \epsilon_{z,p})^2} \\
\epsilon_{et} &= \frac{\sqrt{2}}{3} \sqrt{(\epsilon_r - \epsilon_\theta)^2 + (\epsilon_r - \epsilon_z)^2 + (\epsilon_\theta - \epsilon_z)^2}
\end{aligned}\right\} \quad \text{(B5)}$$

Then by squaring and adding the equations in (B1) and (B3), it follows that

$$\left.\begin{aligned}
K_1 &= \frac{3}{2} \frac{\epsilon_{et}}{\sigma_e} \\
K_2 &= \frac{3}{2} \frac{\epsilon_{ep}}{\sigma_e}
\end{aligned}\right\} \quad \text{(B6)}$$

Hence, by the relation between K_1 and K_2 in equation (B4),

$$\epsilon_{et} = \frac{2}{3} \frac{\sigma_e}{E} (1 + \mu) + \epsilon_{ep} \quad \text{(B7)}$$

The plastic strains can be determined in terms of the total strains by dividing equation (B3) by equations (B1) and applying equations (B6):

$$\frac{\epsilon_{r,p} - \epsilon_{\theta,p}}{\epsilon_r - \epsilon_\theta} = \frac{\epsilon_{r,p} - \epsilon_{z,p}}{\epsilon_r - \epsilon_z} = \frac{\epsilon_{\theta,p} - \epsilon_{z,p}}{\epsilon_\theta - \epsilon_z} = \frac{K_2}{K_1} = \frac{\epsilon_{ep}}{\epsilon_{et}} \quad \text{(B8)}$$

Solving equation (B8) together with the incompressibility relation in equation (B1) results in equations (8) in the text.

Figure 1 shows a typical stress-strain curve for Inconel X and illustrates the meaning of some of the preceding terms.

APPENDIX C

ANALYSIS OF SPHERE

The assumptions in the body of the report for the analysis of the cylinder and the introductory paragraph of appendix A apply to the analysis of the sphere except where by nature of geometry they apply only to the cylinder. The equilibrium equation for a hollow sphere is

$$\frac{d\sigma_r}{dr} + \frac{2(\sigma_r - \sigma_\theta)}{r} = 0 \tag{C1}$$

Because of symmetry, the stress-strain displacement equations reduce to

$$\epsilon_r = \frac{du}{dr} = \frac{1}{E}(\sigma_r - 2\mu\sigma_\theta) + \alpha T + \epsilon_{r,p} \tag{C2}$$

$$\epsilon_\theta = \frac{u}{r} = \frac{1}{E}\left[\sigma_\theta(1 - \mu) - \mu\sigma_r\right] + \alpha T + \epsilon_{\theta,p} \tag{C3}$$

Eliminating u between (C2) and (C3) and introducing the incompressibility condition ($\epsilon_{r,p} + \epsilon_{\theta,p} + \epsilon_{z,p} = 0$) give the compatibility equation:

$$\frac{d}{dr}\left(\frac{\sigma_\theta}{E}\right) - \frac{d}{dr}\left(\frac{\mu\sigma_\theta}{E}\right) - \frac{d}{dr}\left(\frac{\mu\sigma_r}{E}\right) + \frac{d}{dr}(\alpha T) + \frac{d}{dr}(\epsilon_{\theta,p}) = \frac{(\sigma_r - \sigma_\theta)(1 + \mu)}{Er} - \frac{3\epsilon_{\theta,p}}{r} \tag{C4}$$

Putting equations (C1) and (C4) in finite-difference form,

$$C_n\sigma_{r,n} - D_n\sigma_{\theta,n} = F_n\sigma_{r,n-1} + G_n\sigma_{\theta,n-1} \tag{C5}$$

$$C'_n\sigma_{r,n} + D'_n\sigma_{\theta,n} = F'_n\sigma_{r,n-1} + G'_n\sigma_{\theta,n-1} + H'_n \tag{C6}$$

where

$$C_n = \frac{1}{h_n} + \frac{1}{r_n} \qquad C'_n = -\frac{1 + \mu}{2E_n r_n} - \frac{\mu}{E_n h_n}$$

$$D_n = \frac{1}{r_n} \qquad D'_n = \frac{1 - \mu}{E_n h_n} + \frac{1 + \mu}{2E_n r_n}$$

$$F_n = \frac{1}{h_n} - \frac{1}{r_{n-1}} \qquad F'_n = \frac{1 + \mu}{2E_{n-1} r_{n-1}} - \frac{\mu}{E_{n-1} h_n}$$

$$G_n = \frac{1}{r_{n-1}} \qquad G'_n = \frac{1 - \mu}{hE_{n-1}} - \frac{1 + \mu}{2E_{n-1}r_{n-1}}$$

$$H'_n = -\frac{(\alpha\Delta T)_n - (\alpha\Delta T)_{n-1}}{h_n} - \frac{\epsilon_{\theta,p,n} - \epsilon_{\theta,p,n-1}}{h_n} - \frac{3}{2}\left[\left(\frac{\epsilon_{\theta,p}}{r}\right)_n + \left(\frac{\epsilon_{\theta,p}}{r}\right)_{n-1}\right]$$

As in appendix A, the stresses at all stations are expressed in terms of the tangential stress at the inner radius:

$$\sigma_{r,n} = A_{r,n}\sigma_{\theta,a} + B_{r,n}$$

$$\sigma_{\theta,n} = A_{\theta,n}\sigma_{\theta,a} + B_{\theta,n}$$

Substituting into equations (C5) and (C6) gives

$$(C_nA_{r,n} - D_nA_{\theta,n} - F_nA_{r,n-1} - G_nA_{\theta,n-1})\sigma_{\theta,a} + (C_nB_{r,n} - D_nB_{\theta,n} - F_nB_{r,n-1} - G_nB_{\theta,n-1}) = 0 \qquad (C7)$$

$$(C'_nA_{r,n} - D'_nA_{\theta,n} - F'_nA_{r,n-1} - G'_nA_{\theta,n-1})\sigma_{\theta,a} + (C'_nB_{r,n} + D'_nB_{\theta,n} - F'_nB_{\theta,n-1} - G'_nB_{\theta,n-1} - H'_n) = 0 \qquad (C8)$$

For equations (C7) and (C8) to be valid for any value of $\sigma_{\theta,a}$, the following must be true:

$$\left.\begin{aligned} C_nA_{r,n} - D_nA_{\theta,n} - F_nA_{r,n-1} - G_nA_{\theta,n-1} &= 0 \\ C_nB_{r,n} - D_nB_{\theta,n} - F_nB_{r,n-1} - G_nB_{\theta,n-1} &= 0 \\ C'_nA_{r,n} + D'_nA_{\theta,n} - F'_nA_{r,n-1} - G'_nA_{\theta,n-1} &= 0 \\ C'_nB_{r,n} + D'_nB_{\theta,n} - F'_nB_{r,n-1} - G'_nB_{\theta,n-1} - H'_n &= 0 \end{aligned}\right\} \qquad (C9)$$

Solving these four equations simultaneously for $A_{r,n}$, $A_{\theta,n}$, $B_{r,n}$, and $B_{\theta,n}$ gives:

$$\left.\begin{aligned} A_{r,n} &= K_n A_{r,n-1} + L_n A_{\theta,n-1} \\ A_{\theta,n} &= K'_n A_{r,n-1} + L'_n A_{\theta,n-1} \\ B_{r,n} &= K_n B_{r,n-1} + L_n B_{\theta,n-1} + M_n \\ B_{\theta,n} &= K'_n B_{r,n-1} + L'_n B_{\theta,n-1} + M'_n \end{aligned}\right\} \qquad (C10)$$

where

$$K_n = \frac{D'_n F_n + D_n F'_n}{C_n D'_n + C'_n D_n} \qquad K'_n = \frac{C_n F'_n - C'_n F_n}{C_n D'_n + C'_n D_n}$$

$$L_n = \frac{G_n D'_n + G'_n D_n}{C_n D'_n + C'_n D_n} \qquad L'_n = \frac{C_n G'_n - C'_n G_n}{C_n D'_n + C'_n D_n}$$

$$M_n = \frac{D_n H'_n}{C_n D'_n + C'_n D_n} \qquad M'_n = \frac{C_n H'_n}{C_n D'_n + C'_n D_n}$$

Applying the boundary conditions as in appendix A gives

$$\sigma_{\theta,a} = -\frac{B_{r,b}}{A_{r,b}} \qquad (C11)$$

(which is identical with eq. (A12)). The procedure for finding the plastic strains and the iteration procedure are the same as in the case of the cylinder. It should be noted that the equation for the equivalent total strain reduces to $\epsilon_{et} = \frac{2}{3}\left|\epsilon_r - \epsilon_\theta\right|$, and equation (C2) can be put in terms of $\epsilon_{\theta,p}$ by using the condition of incompressibility,

$$\epsilon_r = \frac{1}{E}(\sigma_r - 2\mu\sigma_\theta) + \alpha T - 2\epsilon_{\theta,p}$$

so that only $\epsilon_{\theta,p}$ need be computed. The equation for $\epsilon_{\theta,p}$ now becomes

$$\epsilon_{\theta,p} = \frac{1}{3}\frac{\epsilon_{ep}}{\epsilon_{et}}(\epsilon_\theta - \epsilon_r)$$

APPENDIX D

CALCULATION OF TEMPERATURE DISTRIBUTION FOR SPHERE

The quantity of heat flow at the surface r is

$$Q = \frac{4}{3}\pi\beta\frac{Q}{V}(r_o^3 - r^3)$$

From this is obtained, with manipulation similar to that in the case of the cylinder,

$$T = -\frac{B_j}{A_j} \pm \sqrt{\left(T_o + \frac{B_j}{A_j}\right)^2 - \frac{2f_s(r)}{A_j}}$$

where

$$f_s(r) \equiv \frac{\beta}{3\gamma}\frac{Q}{V}\left(\frac{r^2}{2} - \frac{3r_o^2}{2} + \frac{r_o^3}{r}\right)$$

and

$$T_o = -\frac{B_j}{A_j} \pm \sqrt{\left(T_i + \frac{B_j}{A_j}\right)^2 + \frac{2f_s(r_i)}{A_j}}$$

REFERENCES

1. Wise, Walter R., Jr.: An Investigation of Strain-Energy Absorption Potential as the Criterion for Determining Optimum Reactor-Vessel Containment Design. NAVORD Rep. 5748, Naval Ord. Lab., June 30, 1958.

2. Manson, S. S.: Determination of Elastic Stresses in Gas-Turbine Disks. NACA Rep. 871, 1947. (Supersedes NACA TN 1279.)

3. Millenson, M. B., and Manson, S. S.: Determination of Stresses in Gas-Turbine Disks Subjected to Plastic Flow and Creep. NACA Rep. 906, 1948. (Supersedes NACA TN 1636.)

4. Mendelson, A., and Manson, S. S.: Practical Solution of Plastic Deformation Problems in the Elastic-Plastic Range. NACA TN 4088, 1957.

TABLE I. - COMPARISON OF STRAINS IN CYLINDRICAL AND SPHERICAL PRESSURE VESSELS

Cylinder pressure load, pr, lb/in.	Sphere pressure load, $\sqrt{2}$ pr, lb/in.	Heat flux, Q/V, w/cc	Cylinder equivalent total strain, $\epsilon_{et,c}$, %	Sphere equivalent total strain, $\epsilon_{et,s}$, %	$\frac{\epsilon_{et,s}}{\epsilon_{et,c}}$, %
18,000	25,400	600	1.10	0.87	79
30,000	42,500	350	1.60	1.18	74
36,000	51,000	250	1.72	1.24	72

TABLE II. - INFLUENCE OF CONDUCTIVITY AND COEFFICIENT OF EXPANSION ON EQUIVALENT TOTAL STRAIN AND TANGENTIAL STRESS

(a) Conductivity

Heat flux, Q/V, w/cc	Conductivity, k	Cylinder		Sphere	
		Equivalent total strain, $\epsilon_{et,c}$, %	Tangential stress, $\sigma_{\theta,c}$, psi	Equivalent total strain, $\epsilon_{et,s}$, %	Tangential stress, $\sigma_{\theta,s}$, psi
Pressure load, pr, 18,000 lb/in.					
50	Lower	0.29	108,000	0.27	93,000
	Inconel	.29	108,000	.27	93,000
	Upper	.28	107,000	.26	93,000
950	Lower	1.86	123,000	0.80	102,000
	Inconel	1.61	122,000	.73	101,000
	Upper	1.45	121,000	.65	100,000
Pressure load, pr, 42,000 lb/in.					
50	Lower	0.74	114,000	0.50	97,000
	Inconel	.71	114,000	.49	97,000
	Upper	.64	112,000	.46	96,000
250	Lower	3.10	138,000	1.02	106,000
	Inconel	2.67	134,000	.94	104,000
	Upper	2.15	130,000	.84	103,000

(b) Coefficient of expansion

Heat flux, Q/V, w/cc	Coefficient of thermal expansion, α	Cylinder		Sphere	
		Equivalent total strain, $\epsilon_{et,c}$, %	Tangential stress, $\sigma_{\theta,c}$, psi	Equivalent total strain, $\epsilon_{et,s}$, %	Tangential stress, $\sigma_{\theta,s}$, psi
Pressure load, pr, 18,000 lb/in.					
50	Lower	0.27	107,000	0.26	93,000
	Inconel	.29	107,000	.27	93,000
	Upper	.30	108,000	.27	93,000
950	Lower	1.22	118,000	0.60	99,000
	Inconel	1.62	123,000	.73	101,000
	Upper	1.77	123,000	.82	102,000
Pressure load, pr, 42,000 lb/in.					
50	Lower	0.61	112,000	0.46	96,000
	Inconel	.70	114,000	.48	97,000
	Upper	.75	114,000	.50	97,000
250	Lower	2.11	132,000	0.79	102,000
	Inconel	2.67	134,000	.94	104,000
	Upper	2.70	134,000	1.03	106,000

TABLE III. - COMPARISON OF STRAINS IN CYLINDER AND IN SPHERE WITH THICKNESS EQUAL TO CYLINDER OPTIMUM

Pressure load, pr, lb/in.	Heat flux, Q/V, w/cc	Thickness, t, in.	Equivalent total strain, ϵ_{et}, %	
			Cylinder	Sphere
18,000	500	0.18	0.95	0.74
30,000	250	.28	1.18	.92
42,000	150	.38	1.45	1.01

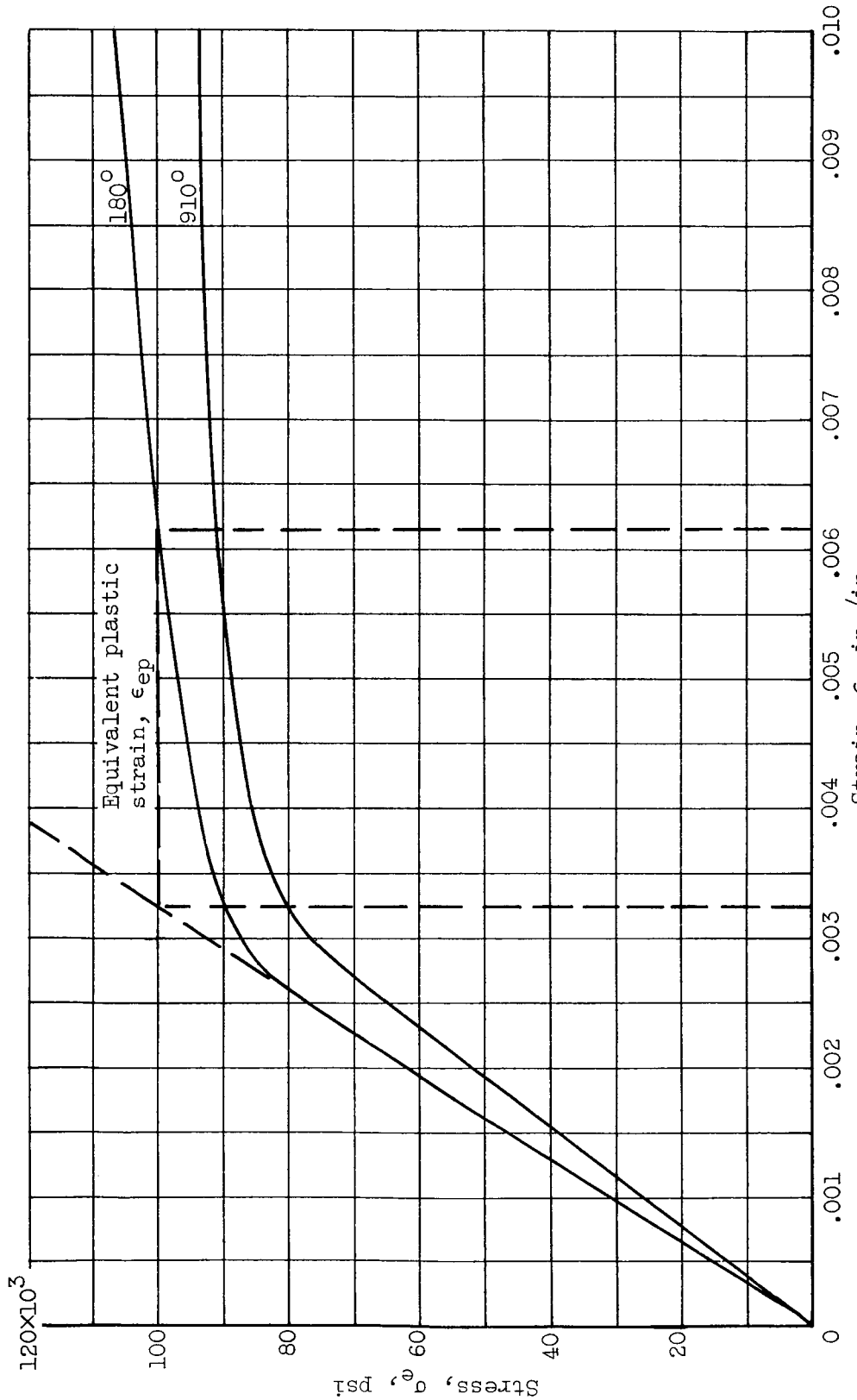

Figure 1. - Stress-strain curve for Inconel X at 180° and 910° F.

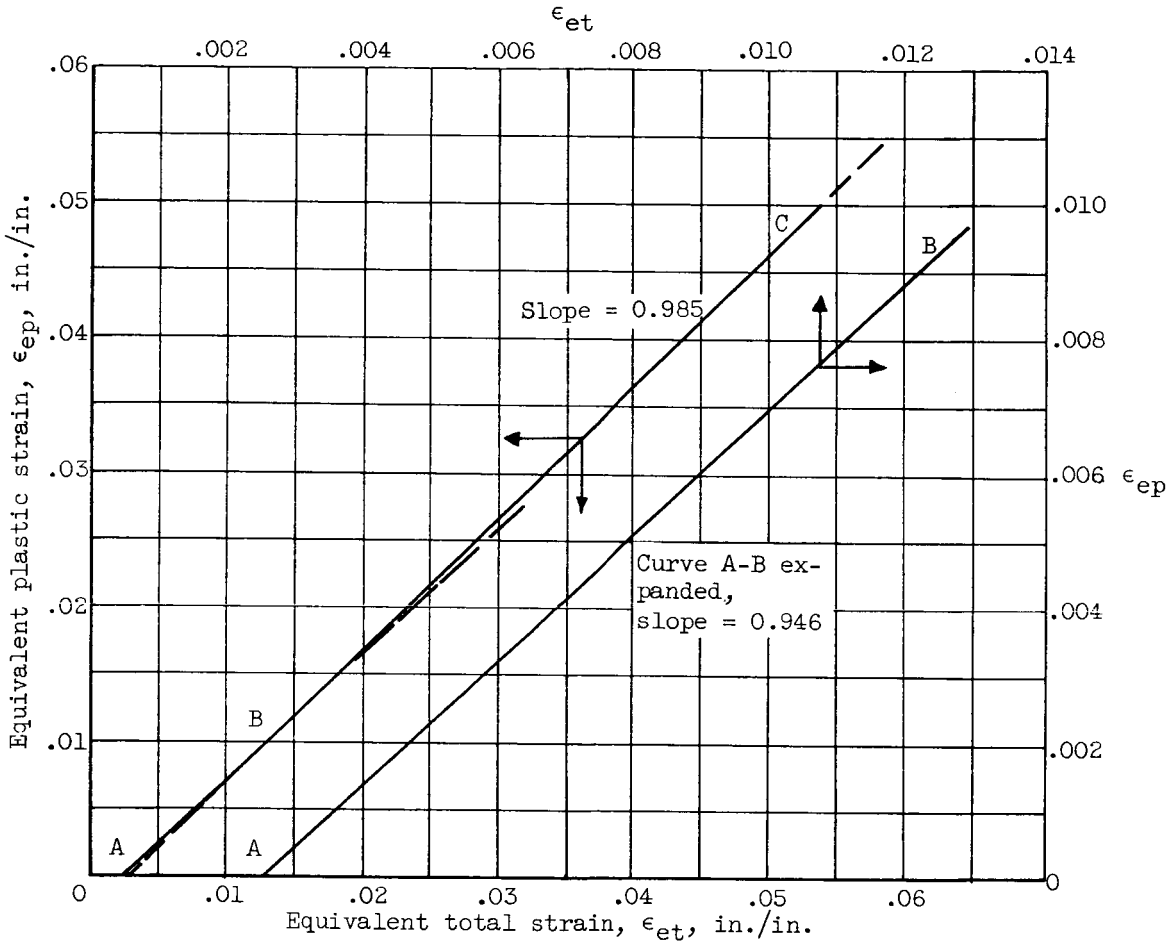

Figure 2. - Relation between equivalent plastic strain and equivalent total strain.

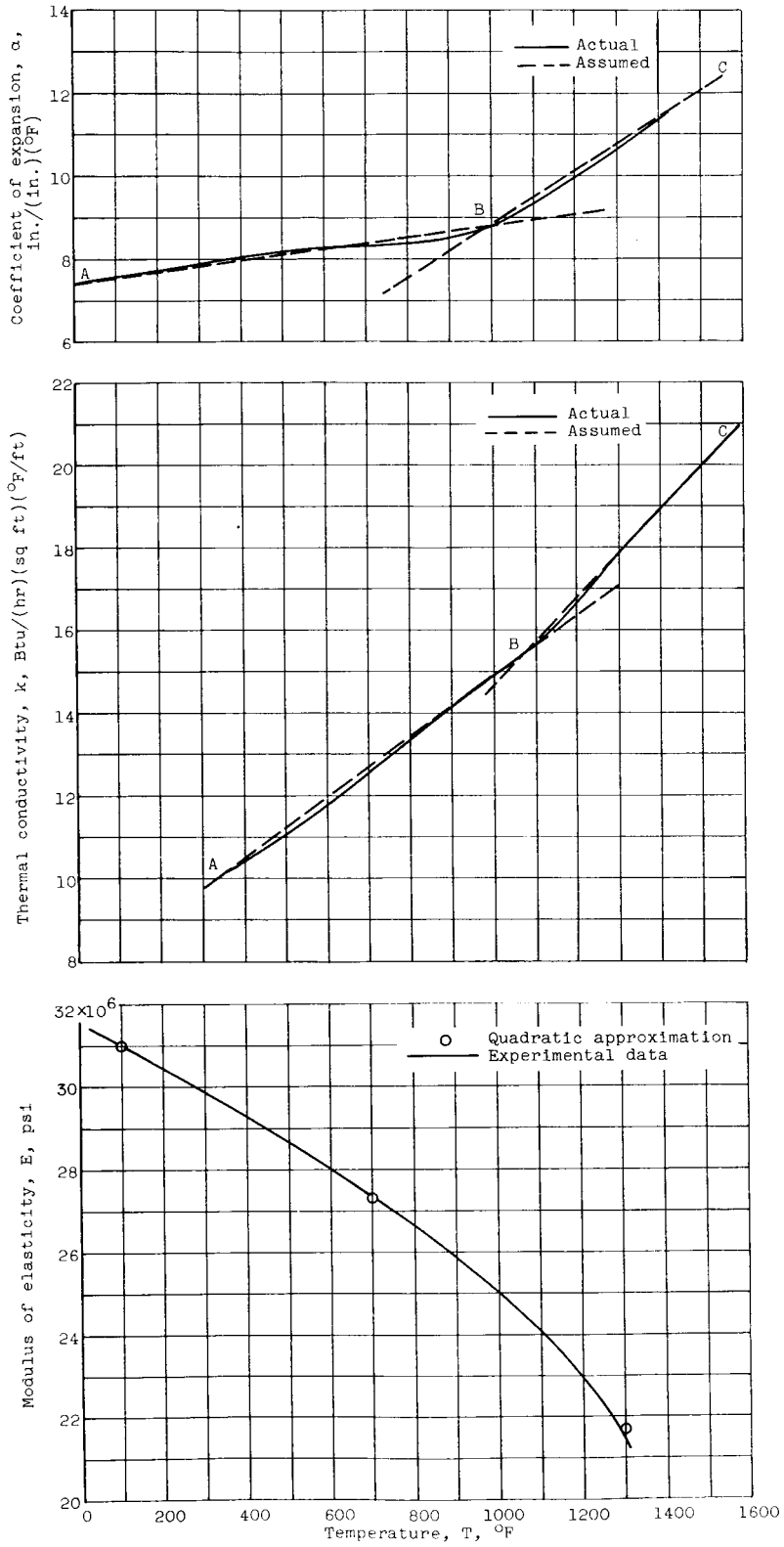

Figure 3. - Variation of material properties with temperature of Inconel X.

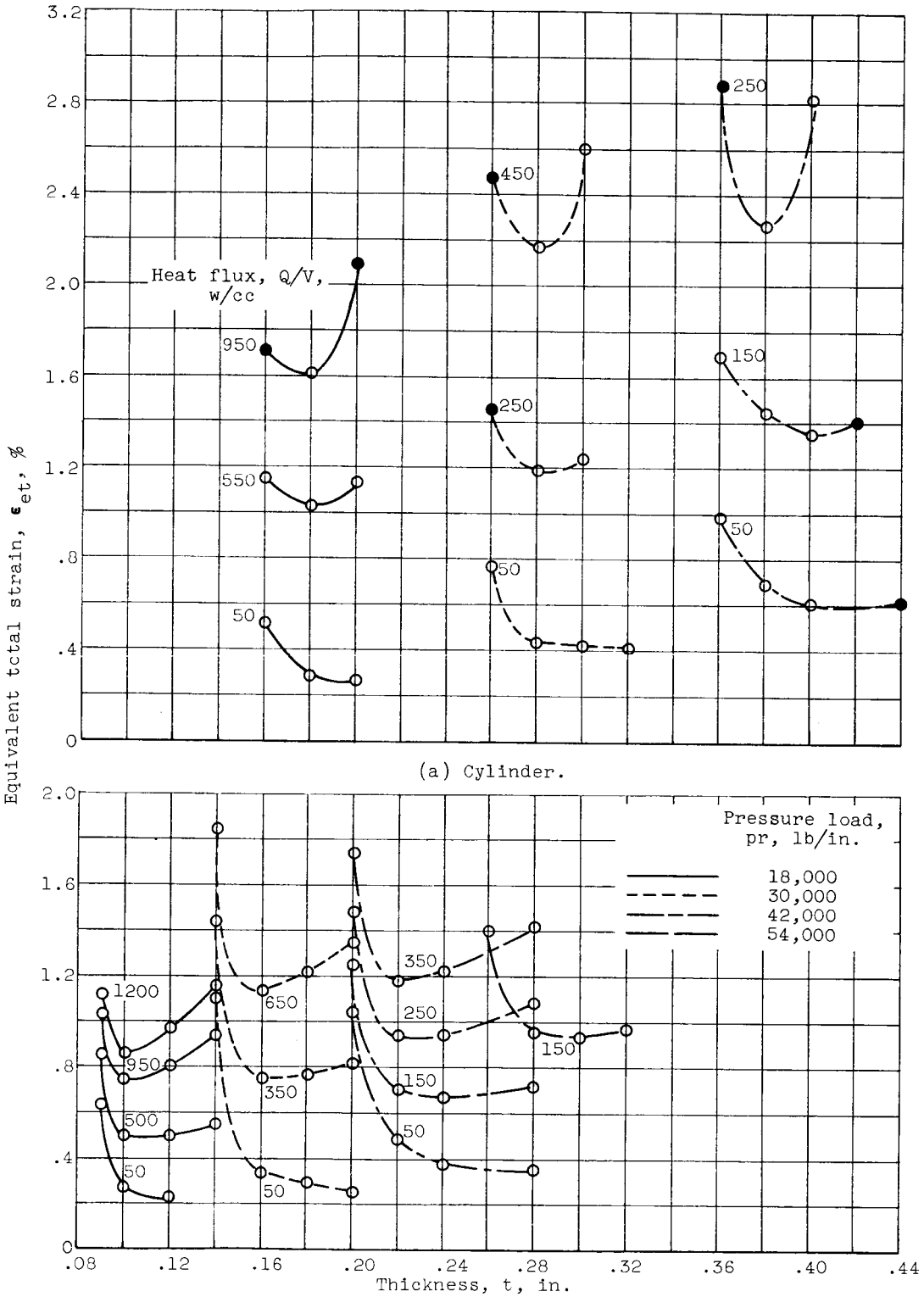

(a) Cylinder.

(b) Sphere.

Figure 4. - Effects of heat flux and pressure load on optimum thickness.

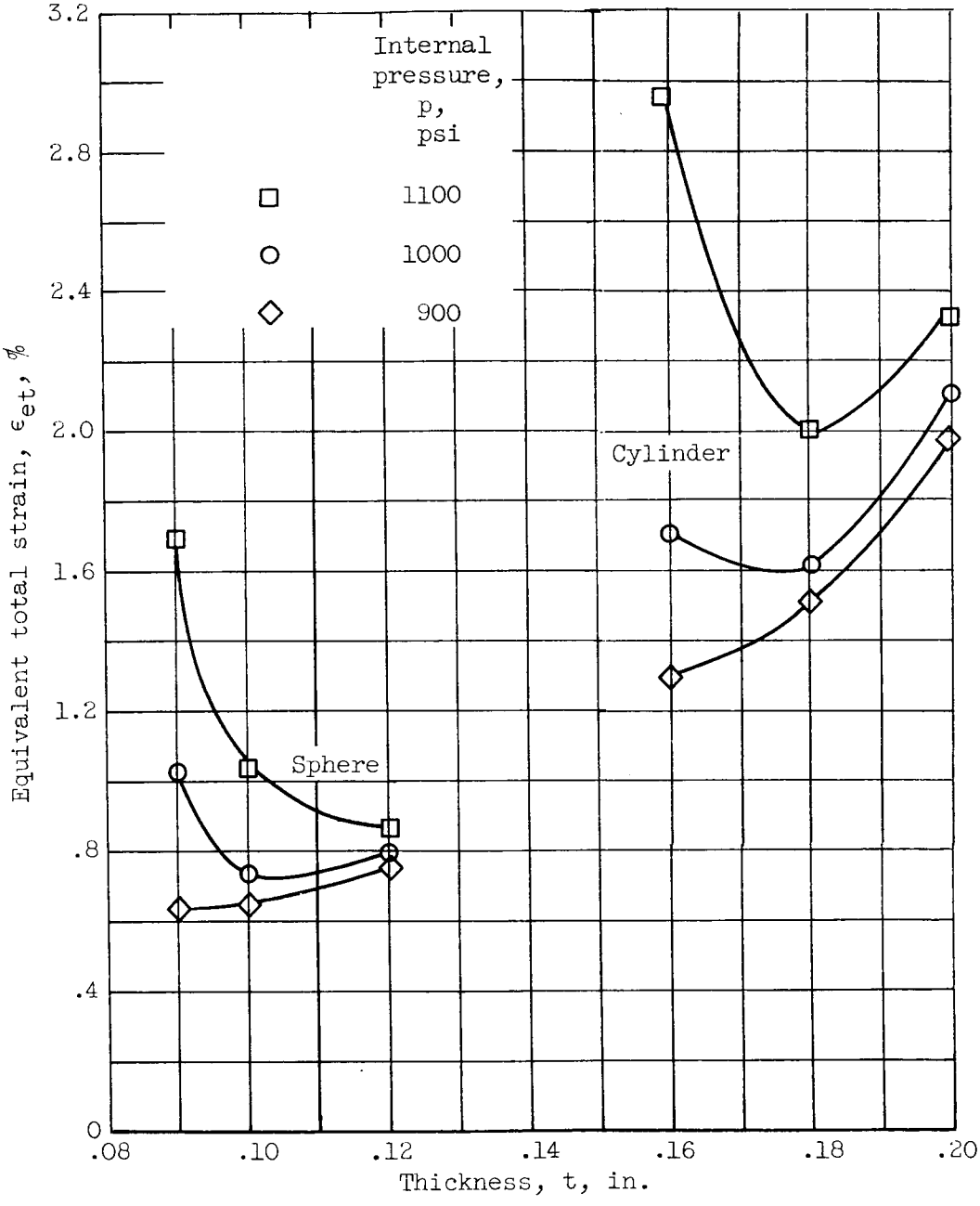

Figure 5. - Effect of pressure excursions on equivalent total strain. Radius, 18 inches; heat flux, 950 watts per cubic centimeter.

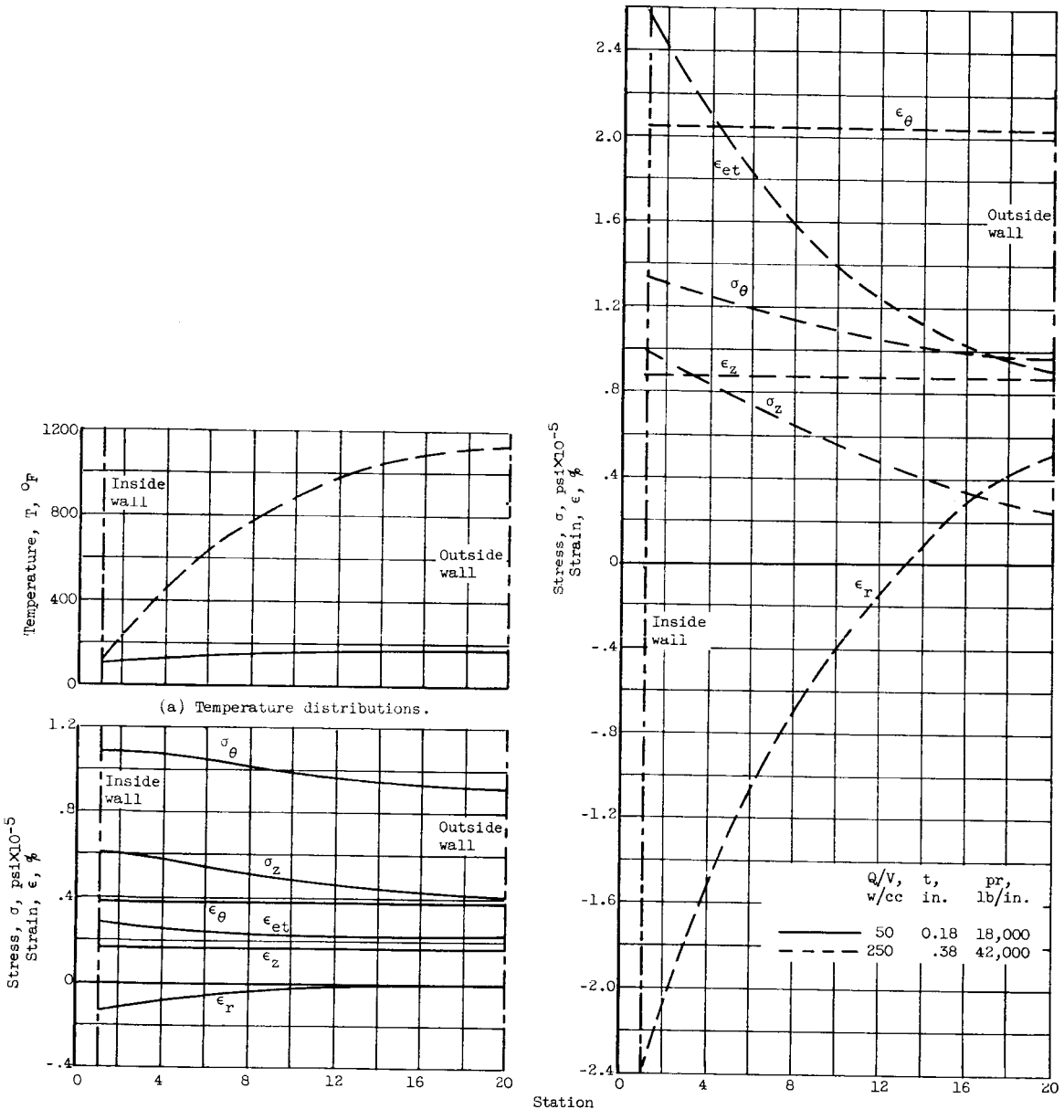

(a) Temperature distributions.

(b) Stress and strain distributions; low-strain condition.

(c) Stress and strain distributions; high-strain condition.

Figure 6. - Temperature and stress-strain distributions in cylindrical pressure vessel.

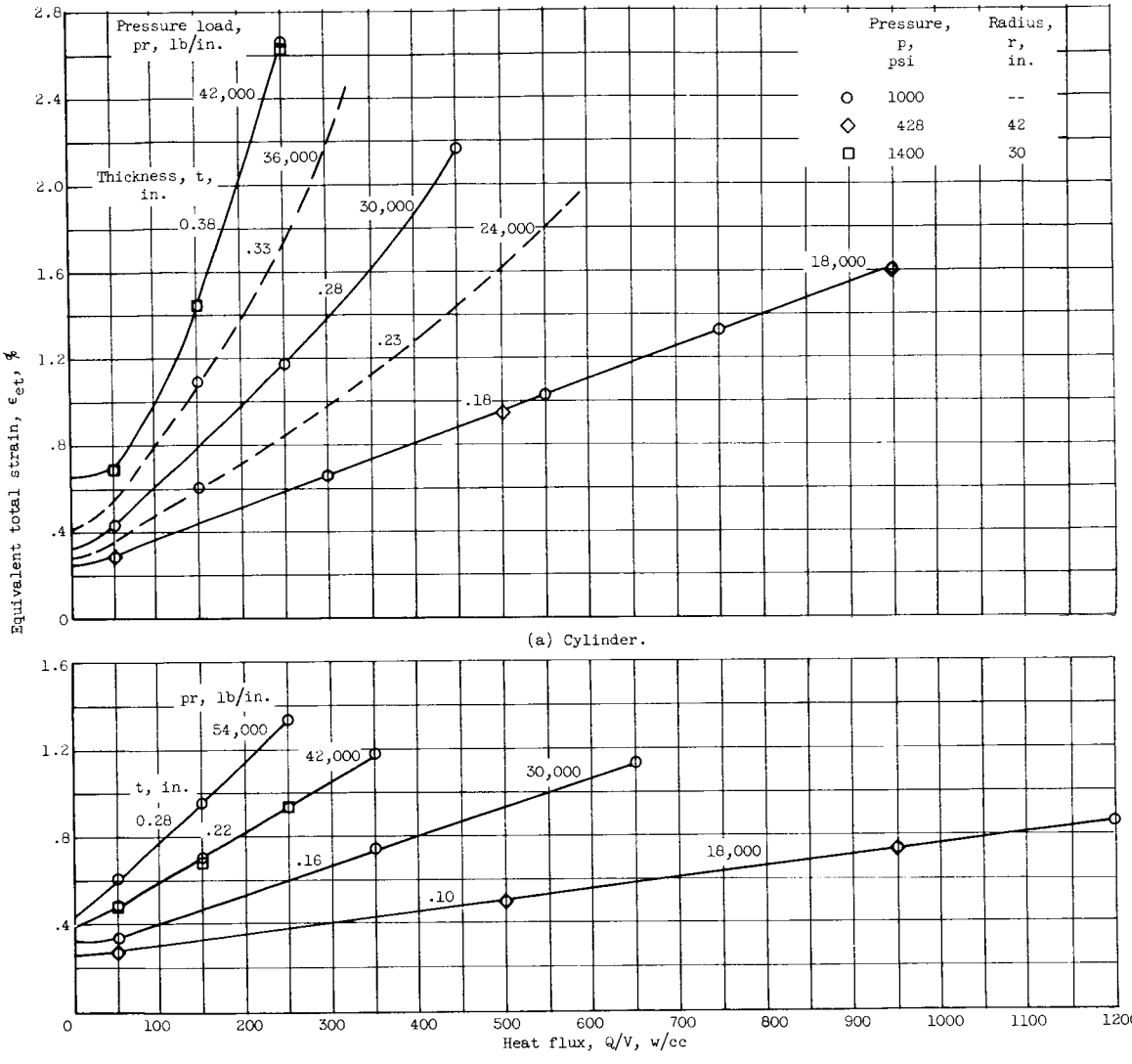

Figure 7. - Effect of heat flux and pressure load on equivalent total strain.